Supplementary Information

Carborane-Modified Polyetherimide Films for High-Temperature Dielectric Applications

Haotian Xiao, [a,b,c#] *Chongwen Yu,* [d#] *Haochen Guo,* [b,c,e] *Zijie Xu,* [f] *Xiaoqing Sun,* [g] *Jian Xu,* [g] *Yujie Song,* [b,c *] *Xiangsheng Meng,* [b,c] *Jingling Yan,* [b,c] *Zhen Wang* [b,c]

[a] University of Chinese Academy of Sciences, Beijing, 100049, China

[b] Laboratory of Polymers and Composites, Ningbo Institute of Materials Technology and Engineering, Chinese Academy of Sciences, Ningbo, 315201, China.

[c] Ningbo Key Laboratory of High-Performance Polymers and Composites, Ningbo, 315201, China.

[d] Jiangxi Key Laboratory of Advanced Ceramic Materials, China National Light Industry Key Laboratory of Functional Ceramic Materials, School of Materials Science and Engineering, Jingdezhen Ceramic University, Jingdezhen 333403, China

[e] School of Materials Science and Engineering, Shanghai University, Shanghai 200444, China.

[f] School of Materials Science and Chemical Engineering, Ningbo University, Ningbo 315211, China

[g] State Key Laboratory of Fine Chemicals, Liaoning High Performance Polymer Engineering Research Center, School of Chemical Engineering, Dalian University of Technology, Dalian, 116024, China.

[#] Haotian Xiao and Chongwen Yu contributed equally to this paper.

[*] Corresponding author: Yujie Song, E-mail: songyujie@nimte.ac.cn

1 Instruments and characterization

The ^{1}H NMR and ^{13}C NMR spectra were recorded on a Bruker AVANCE NEO spectrometer, using tetramethylsilane (TMS) as an internal standard. Samples were tested in either 0.5 mL deuterated chloroform (Chloroform-D) at a temperature of 25 ℃.

The Fourier transform infrared (FT-IR) spectra were collected on a Bruker INVENIOR FT-IR spectrometer, using the attenuated total reflectance (ATR) mode, within the spectral range of 4000-500 cm^{-1}, with 64 scans.

The thermogravimetric analysis (TGA) was performed on a Netzsch STA449F3 instrument under argon or air atmosphere with a flow rate of 20 mL min^{-1}, in the temperature range of 50 ℃ to 1010 ℃, at a heating rate of 10 ℃ min^{-1}.

The differential scanning calorimetry (DSC) was conducted on a TA Q250 instrument under a nitrogen atmosphere with a flow rate of 20 mL min^{-1}, in the temperature range of 50 °C to 400 °C, at a heating rate of 10°C min^{-1}.

The liquid chromatography-quadrupole time-of-flight mass spectrometer (LC-Q-TOF) was performed on an AB Sciex 4600 with positive and negative ion modes.

The Specific heat capacity measurements were performed on a TA Instruments Discovery DSC 250 differential scanning calorimeter, using synthetic sapphire (α-Al_2O_3) as the standard reference material. Samples, encapsulated in hermetic aluminum pans, were tested under a dry nitrogen atmosphere (flow rate: 50 mL/min) over a temperature range of 25 ℃ to 100 ℃ at a heating rate of 10 ℃/min.

The density of the thin films was determined using a Mettler Toledo XS205 DualRange analytical balance equipped with a dedicated density determination kit. Ethanol at 25 ℃ served as the immersion liquid. Film samples, cut into specific dimensions (e.g., 40 mm × 40 mm), were mounted on the specialized film sample holder and submerged in the liquid during measurement. The density was calculated according to the formula using measurements obtained from a density balance: dry weight, buoyant weight (weight in liquid), and saturated weight.

$$\rho_{object} = \left(\frac{W_{dry}}{W_{wet} - W_{submerge}} \right) \times \rho_{fluid}$$

The thermal conductivity of the thin films was determined using a Netzsch LFA 467 HyperFlash laser flash apparatus. Samples were prepared by coating the film surface with a thin layer of graphite spray to enhance laser absorption and infrared emissivity. Measurements were conducted on a sandwich structure (film adhered to an opaque reference substrate, e.g., fused silica or sapphire) at temperatures ranging from 25 °C to 150 °C under a dynamic argon atmosphere.

Thermal conductivity (λ) was calculated using the relationship $\lambda = \alpha \cdot \rho \cdot c_p$.

The frequency-dependent dielectric properties of the samples were characterized using a Novocontrol broadband dielectric spectrometer. Before testing, circular gold electrodes (13 mm diameter) were deposited onto both surfaces of the films, with a nominal thickness of approximately 100 nm. An alternating current (AC) voltage of 3 V was applied across the film, and the ε_r and tan δ were measured at room temperature over the frequency range of 10^0 to 10^7 Hz.

The temperature-dependent dielectric properties of the samples were characterized using a Biolin DMS500 temperature-variable dielectric spectrometer. Before testing, aluminum electrodes with a diameter of approximately 9 mm were vacuum deposited onto both surfaces of the films. Measurements of the ε_r and tan δ were conducted at a frequency of 1 kHz during heating from 20 °C to 200 °C at a constant rate of 1 °C/min.

Fractional free volume(FFV) analysis was conducted using the Forcite module within Materials Studio 2019. The Universal force field, validated for organic and hybrid systems, was employed throughout the simulations. Initial structural optimization utilized the Smart algorithm, combining steepest descent and conjugate gradient methods, with convergence criteria set to an energy change below 1×10^{-4} kcal/mol and forces below 0.001 kcal/mol/Å. Following optimization, systems underwent equilibration under NPT ensemble conditions at 298 K and 1 atm using the Berendsen thermostat and barostat with a 0.1 ps time constant. Molecular dynamics

simulations proceeded for 500 ps until density fluctuations stabilized within ±0.01 g/cm^3. FFV was subsequently calculated via the Atom Volumes & Surfaces tool. This method deployed a spherical probe of radius 0.1 nm to map probe-accessible regions based on the Connolly surface definition. FFV values were computed as the ratio of probe-accessible volume to the total cell volume.

Breakdown voltage testing was performed using an automatic voltage endurance tester (LJC-100KV). Five specimens were cut from each film for measurement.

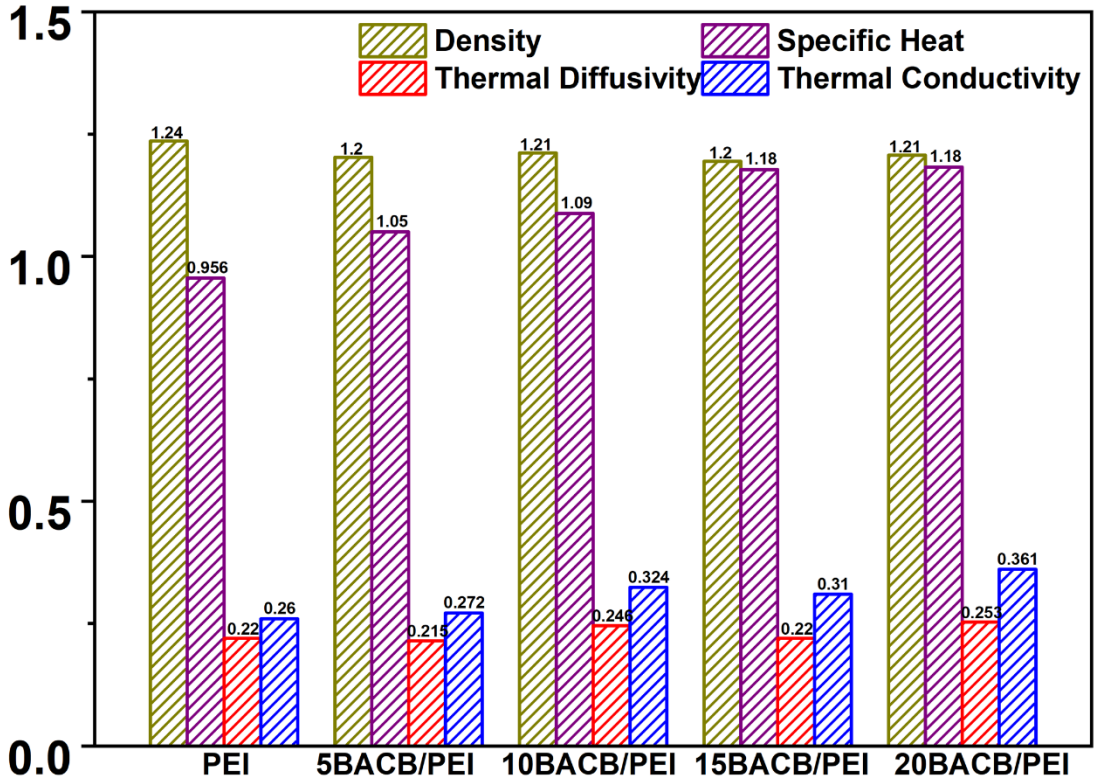

Figure S1 Density, specific heat capacity, thermal diffusivity, and thermal conductivity of the *x*BACB/PEI films.

Table S1 Formulations, Density, Specific Heat, Thermal Diffusivity, and Thermal Conductivity Results of *x*BACB/PEI.

Sample	Density(kg/m^3)	Specific Heat (J/kg•°C)	Thermal Diffusivity (W/m^2·K)	Thermal Conductivity (W/m·K)
PEI	1.24	0.956	0.220	0.260
5BACB/PEI	1.20	1.050	0.215	0.272
10BACB/PEI	1.21	1.090	0.246	0.324
15BACB/PEI	1.12	1.180	0.220	0.310
20BACB/PEI	1.21	1.180	0.253	0.361

2 Monomer synthesis

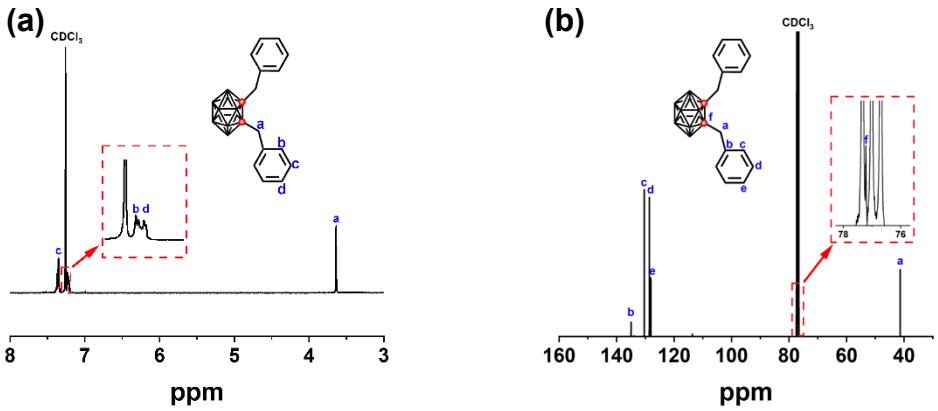

Figure. S2 (a) ^{1}H NMR spectrum; (b) ^{13}C NMR spectrum of 1,2-Dibenzyl-*o*-carborane.

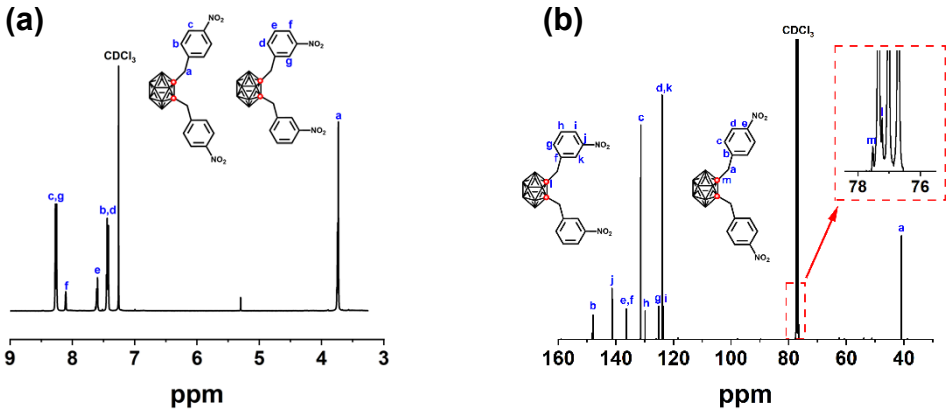

Figure. S3 (a) ^{1}H NMR spectrum; (b) ^{13}C NMR spectrum of 1,2-Dibenzylnitro-*o*-carborane

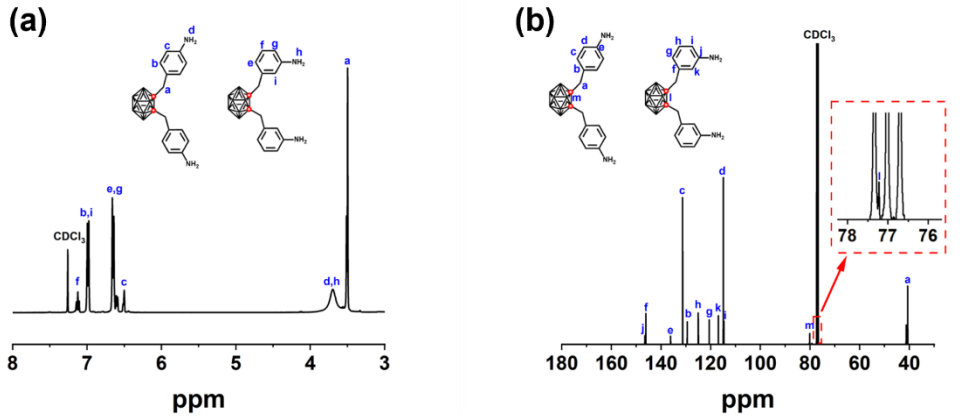

Figure. S4 (a) ^{1}H NMR spectrum; (b) ^{13}C NMR spectrum of 1,2-Dibenzylamino-*o*-carborane

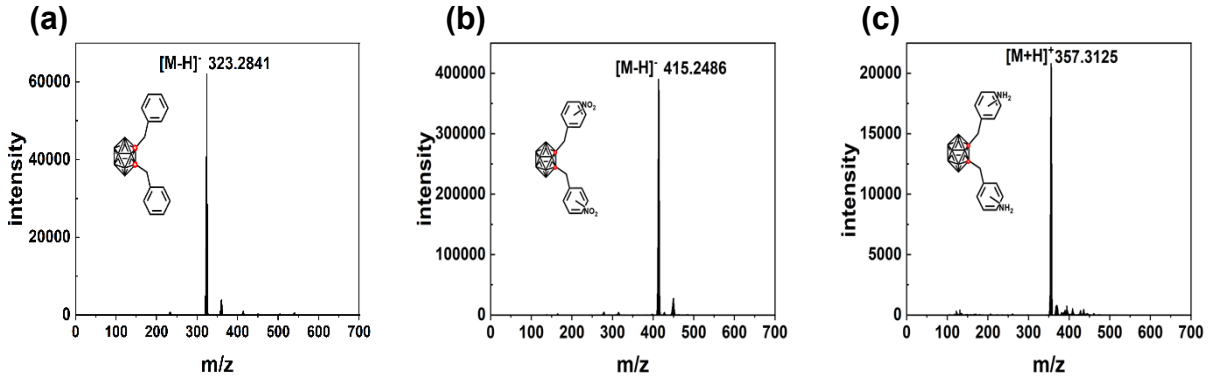

Figure. S5 LC-Q-TOF spectra of (a) 1,2-Dibenzyl-*o*-carborane; (b) 1,2-Dibenzylnitro-*o*-carborane; (c) 1,2-Dibenzylamino-*o*-carborane.

3 Polymer synthesis

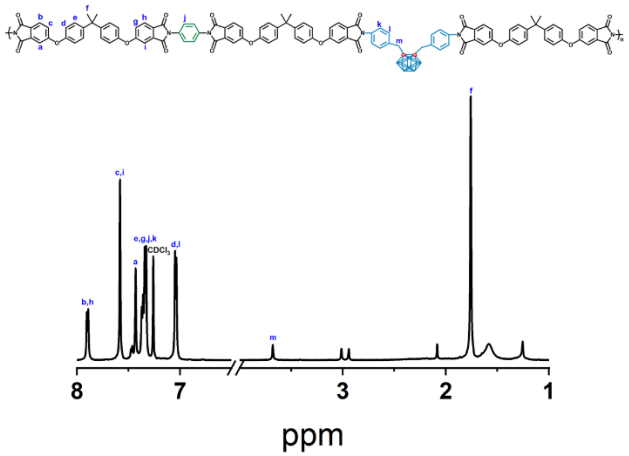

Figure. S6 ^{1}H NMR spectrum of *x*BACB/PEI.

4 Film flexibility

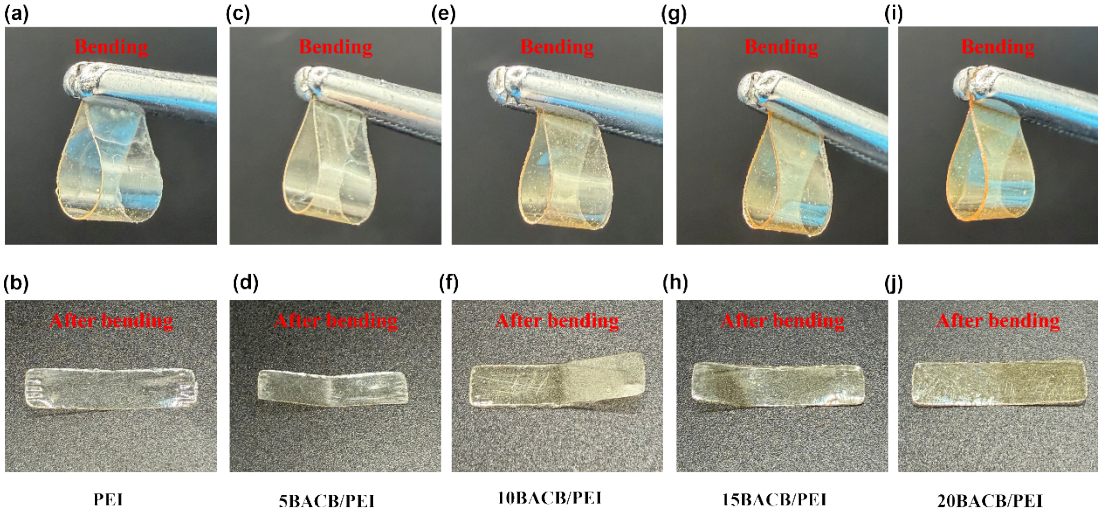

Figure. S7 Digital photographs of *x*BACB/PEI films (x = 0, 5, 10, 15, and 20 wt%) in a bent state.